Molecular Therapy
Original Article

hucMSC Exosome-Derived GPX1 Is Required for the Recovery of Hepatic Oxidant Injury

Yongmin Yan,[1,4] Wenqian Jiang,[1,4] Youwen Tan,[2] Shengqiang Zou,[2] Hongguang Zhang,[2] Fei Mao,[1] Aihua Gong,[1] Hui Qian,[1,3] and Wenrong Xu[1,3]

[1]Liver Disease and Cancer Institute, School of Medicine, Jiangsu University, 212013 Zhenjiang, Jiangsu, People's Republic of China; [2]The Affiliated Third Hospital of Zhenjiang, Jiangsu University, 212013 Zhenjiang, Jiangsu, People's Republic of China; [3]Key Laboratory of Laboratory Medicine of Jiangsu Province, School of Medicine, Jiangsu University, 212013 Zhenjiang, Jiangsu, People's Republic of China

Exosomes are small biological membrane vesicles secreted by various cells, including mesenchymal stem cells (MSCs). We previously reported that MSC-derived exosomes (MSC-Ex) can elicit hepatoprotective effects against toxicant-induced injury. However, the success of MSC-Ex-based therapy for treatment of liver diseases and the underlying mechanisms have not been well characterized. We used human umbilical cord MSC-derived exosome (hucMSC-Ex) administrated by tail vein or oral gavage at different doses and, in engrafted liver mouse models, noted antioxidant and anti-apoptotic effects and rescue from liver failure. A single systemic administration of hucMSC-Ex (16 mg/kg) effectively rescued the recipient mice from carbon tetrachloride (CCl_4)-induced liver failure. Moreover, hucMSC-Ex-derived glutathione peroxidase1 (GPX1), which detoxifies CCl_4 and H_2O_2, reduced oxidative stress and apoptosis. Knockdown of GPX1 in hucMSCs abrogated antioxidant and anti-apoptotic abilities of hucMSC-Ex and diminished the hepatoprotective effects of hucMSC-Ex in vitro and in vivo. Thus, hucMSC-Ex promote the recovery of hepatic oxidant injury through the delivery of GPX1.

INTRODUCTION

Liver injury often occurs in response to various chronic injuries, such as viral hepatitis, alcohol, drugs, metabolic diseases, and autoimmune hepatic cell insult. Drug- and toxicant-induced liver injury is a major reason for liver transplantation, and at present, no ideal treatments are available for liver injury.[1] Thus, better therapies are needed to prevent additional hepatic damage.

Increasing evidence shows that mesenchymal stem cell (MSC) transplantation may be a promising new therapeutic approach for treating liver injury. Currently, approximately 36 MSC-based clinical trials are being conducted for different types of liver injuries, such as autoimmune hepatitis, alcoholic liver cirrhosis, and liver fibrosis. Human umbilical cord is a transplantable source of MSCs and human umbilical cord-derived MSCs (hucMSCs) are of interest in regenerative medicine for liver injury because of low cost, minimal invasiveness, convenient isolation, low immunogenicity and immunomodulatory activity, and differentiation multipotency.[2–4] Results from phase I and II clinical studies of hucMSC transplantation for patients with decompensated liver cirrhosis showed that hucMSCs may improve liver function and clinical symptoms (https://ClinicalTrials.gov identifier NCT0134225).

Although advances in hucMSC transplantation offer great potential for treating liver injury, long-term safety is a concern.[5] Recent work suggests that transplantation of native MSCs can alleviate liver injury through paracrine effects.[6] MSC-derived exosomes (MSC-Ex), membrane-enclosed vesicles found in MSC-conditioned medium (MSC-CM), have been reported to contribute to angiogenesis, neurite outgrowth, and skeletal muscle regeneration.[7–9] We previously demonstrated that hucMSCs and hucMSC-Ex could alleviate liver fibrosis, promote liver and renal injury repair, and improve wound healing.[10–12] hucMSC-Ex may have similar protective and reparative properties as their cellular counterparts in tissue repair.[13] Compared with MSC transplantation, hucMSC-Ex therapies are preferred because of fewer immune responses; increased safety; and ease of storage, shipment, and administration.[13] Therefore, hucMSC-Ex may be ideal for treating liver injuries and diseases, but mechanisms underlying their therapeutic effects are unclear.

Exosomes contain functional mRNA, microRNA, and proteins that can alter the cellular environment to enhance tissue repair.[12,14] Thus, it is necessary to determine key factors in hucMSC-Ex that mediate hepatoprotective effects. Oxidative stress is often involved in liver diseases and may contribute to the development of viral hepatitis, alcoholic liver disease, non-alcoholic steatohepatitis (NASH), Wilson's disease, and hepatocellular carcinoma (HCC).[15–19] Antioxidant therapy has been considered for treatment of liver diseases, and previous work suggests that transplanted MSCs can restore liver function.[6,20] However, how MSC-Ex modulate oxidative stress in liver injury repair is unclear. Glutathione peroxidase 1 (GPX1), a critical

Received 21 July 2016; accepted 27 November 2016;
http://dx.doi.org/10.1016/j.ymthe.2016.11.019.

[4]These authors contributed equally to this work.

Correspondence: Yongmin Yan, School of Medicine, Jiangsu University, 301 Xuefu Road, 212013 Zhenjiang, Jiangsu, People's Republic of China.
E-mail: ujsyym@163.com
Correspondence: Wenrong Xu, School of Medicine, Jiangsu University, 301 Xuefu Road, 212013 Zhenjiang, Jiangsu, People's Republic of China.
E-mail: icls@ujs.edu.cn

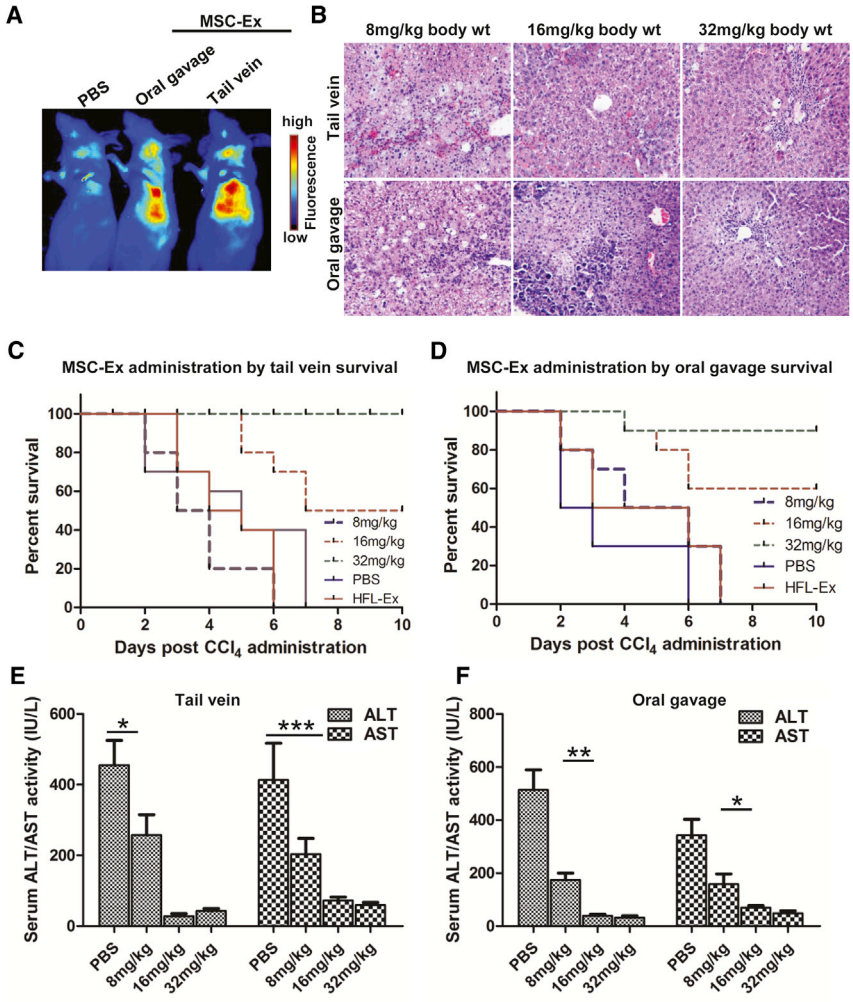

Figure 1. hucMSC-Ex Rescued CCl_4-Induced Liver Failure

(A) Distribution of CM-Dir labeled hucMSC-Ex in CCl_4-injured mice after tail vein or oral gavage administration according to in vivo fluorescent imaging 24 hr post-treatment. (B) Representative images of H&E staining after hucMSC-Ex treatment (8, 16, and 32 mg/kg) significantly inhibited hepatocyte denaturation and hepatic lobule destruction in mouse livers 72 hr after hucMSC-Ex treatment. Original magnification 200×. (C and D) Survival curves of CCl_4-injured mice treated with hucMSC-Ex by tail vein (C) or oral gavage (D) 8–32 mg/kg. hucMSC-Ex administration dose-dependently rescued recipient animals from liver failure. (tail vein-administered HFL-Ex 32 mg/kg body weight versus MSC-Ex 16 mg/kg body weight: n = 10, $p < 0.01$; oral gavage-administered HFL-Ex 32 mg/kg body weight versus MSC-Ex 16 mg/kg body weight: n = 10, $p < 0.01$). (E and F) Serum alanine ALT and AST are reduced in hucMSC-Ex-treated mice 72 hr after tail vein or oral gavage treatment (n = 5; *$p < 0.05$, **$p < 0.01$, ***$p < 0.001$).

human antioxidant,[21] detoxifies hydrogen peroxide and upregulates GPX1 activity to promote cell survival, but whether hucMSC-Ex-mediated delivery of GPX1 can restore liver function is unknown.

In this study, we assessed the use of hucMSC-Ex for treatment of liver disease and assessed efficacy and mechanism of action. Antioxidant and anti-apoptotic effects of hucMSCs-Ex on CCl_4- and H_2O_2-induced hepatic injury in vitro and in vivo were also investigated, and hucMSC-Ex-derived GPX1 promoted detoxification of CCl_4 and H_2O_2 and inhibited oxidative stress and apoptosis in vitro and in vivo. Our results provide a better understanding for using hucMSC-Ex for treating liver injury.

RESULTS

hucMSC-Ex Rescued CCl_4-Induced Liver Failure

To evaluate the lethality of CCl_4 in mice, CCl_4/kg (0.15–0.35 mL, intraperitoneal) was tested for hepatotoxicity and lethality. CCl_4 at 0.15 and 0.2 mL/kg body weight did not induce sufficient lethality, but 0.3 and 0.35 mL/kg body weight caused rapid death. Thus, 0.25 mL/kg was used for subsequent experiments (Figure S1). hucMSC-Ex was prepared and purified as described previously.[22] Nanoparticle tracking analysis (NTA) and transmission electron microscopy (TEM) analyses confirmed spheroid morphology of hucMSC-Ex (diameter 30–100 nm; Figures S2A and S2B). Western blot results confirmed expression of exosomal markers CD9, CD61, and CD63 in hucMSC-Ex (Figure S2C). In vivo fluorescent imaging and human CD63 staining results showed that CM-Dir-labeled hucMSC-Ex administered by tail vein or oral gavage targeted injured and normal livers at 24 hr post-injection (Figures 1A, S3A, and S3B). Hematoxylin and eosin (H&E) staining confirmed large areas of fatty degeneration and portal hepatocyte necrosis after PBS and 8 mg/kg hucMSC-Ex treatment, while 16 and 32 mg/kg hucMSC-Ex significantly inhibited hepatocyte denaturation and hepatic lobule destruction (Figures 1B and S4).

To assess the therapeutic potential of hucMSC-Ex, 8, 16, and 32 mg/kg (tail vein or oral gavage) was given 24 hr after the administration of CCl_4. For the tail vein administration of hucMSC-Ex, all animals infused with 8 mg/kg died of liver failure, and half survived after treatment with 16 mg/kg. All mice were rescued by 32 mg/kg hucMSC-Ex (Figure 1C). A dose-dependent effect was also observed after treatment with hucMSC-Ex from oral gavage administration of hucMSC-Ex. Specifically, 8 mg/kg hucMSC-Ex failed to rescue recipient animals from liver failure, but 60% and 90% of mice recovered from 16 and 32 mg/kg of hucMSC-Ex treatment, respectively (Figure 1D). Also, serum ALT (alanine aminotransferase) and AST (aspartate aminotransferase) decreased in animals given 8 mg/kg hucMSC-Ex at 72 hr post-injection, confirming that hucMSC-Ex reduced acute extensive liver injury by CCl_4 (Figures 1E and 1F; n = 5; *$p < 0.05$, **$p < 0.01$, ***$p < 0.001$).

hucMSC-Ex Reduced Oxidative Stress in Mice

CCl_4 induces hepatotoxic effects via the CYP 450-dependent monooxygenase system to release reactive free radicals, and hucMSC-Ex had antioxidant effects on CCl_4-induced liver failure. To illustrate the antioxidant effects of hucMSC-Ex, human lung fibroblast (HFL-1)-derived exosomes (HFL-Ex) were used as controls. First, reactive oxygen species (ROS) were measured in hepatocytes isolated from hucMSC-Ex-treated livers using a DCF-DA probe. Imaging flow cytometry indicated that the percentage of DCF-positive cells and fluorescent intensity decreased after hucMSC-Ex treatment (Figures 2Ai and 2Aii; n = 4; $^{**}p < 0.01$). The oxidative stress product 8-OHdG and TUNEL-positive cells were decreased in hucMSC-Ex cells compared with PBS and HFL-Ex groups (Figures 2B and 2C; n = 3; $^{*}p < 0.05$, $^{**}p < 0.01$, $^{***}p < 0.001$). MDA was also reduced in the hucMSC-Ex group (Figure 2D; n = 3; $^{*}p < 0.05$). Luminex analysis confirmed that pro-inflammatory cytokines (G-CSF, interleukin [IL]-1α, IL-6, monocyte chemoattractant protein-1 [MCP-1], and tumor necrosis factor-α [TNF-α]) were reduced in the hucMSC-Ex group (Figure 2E; n = 3; $^{*}p < 0.05$, $^{**}p < 0.01$). Thus, hucMSC-Ex can inhibit oxidative stress and apoptosis in CCl_4-injured mouse livers and promote hepatic recovery.

hucMSC-Ex Reduced Oxidative Stress in CCl_4- and H_2O_2-Injured L02 Liver Cells

To measure distribution of exosomes in L02 cells, exosomes and L02 cells were labeled with fluorescent carbocyanine dyes CM-Dil (red) and CM-Dio (green) respectively. After 24 hr co-incubation, the uptake efficiency was measured by imaging flow cytometry, and results showed that ~75% of cells were double-stained (Figure 3Ai), the CM-Dil labeled HFL-Ex and hucMSC-Ex could be imaged in L02 cells (Figure 3Aii).

CCl_4 and H_2O_2 treatment-induced ROS, oxidative stress, and hepatotoxicity[20,23] was assessed by measuring antioxidant activity with DCF-DA 24 hr after hucMSC-Ex co-incubation. ROS were decreased after treatment with MSC-conditioned medium (MSC-CM) and hucMSC-Ex compared with HFL-conditional medium (HFL-CM), HFL-Ex, and PBS (Figure 3B; n = 5; $^{***}p < 0.001$). MDA level was also reduced in MSC-CM and hucMSC-Ex groups (Figure 3C; n = 3; $^{***}p < 0.001$). We next assessed the effect of hucMSC-Ex on hepatocytes survival. Cell viability were reduced in CCl_4- and H_2O_2-injured L02 cells, and were increased in a dose-dependent fashion in hucMSC-Ex-treated cells. In contrast, HFL-Ex had little effect on cell viability (Figure 3D). Thus, hucMSC-Ex may have antioxidant activity that can improve cell viability.

hucMSC-Ex Inhibited Oxidative Stress-Induced Apoptosis

Oxidative stress can induce hepatic apoptosis.[24] We found that at 24 hr after treatment, apoptotic cells decreased (2-fold) in the hucMSC-Ex group compared with the PBS and HFL-Ex groups (Figure 4A; n = 3; $^{*}p < 0.05$, $^{**}p < 0.01$). Hoechst 33342 staining revealed fewer apoptotic cells (half-moon nuclei) in the hucMSC-Ex group compared with the PBS and HFL-Ex groups (Figure 4B; n = 3; $^{*}p < 0.05$, $^{**}p < 0.01$).

Mitochondria can undergo apoptosis because of oxidative stress.[24] Thus, we measured changes in mitochondrial membrane potential in L02 cells treated with or without hucMSC-Ex using JC-1 staining. More cells were fluorescent green in the PBS and HFL-Ex groups, but more cells were fluorescent red in the hucMSC-Ex group (Figure 4Ci). The ratio of green to red fluorescence was significantly decreased in L02 cells treated with hucMSC-Ex, indicating a reversal of oxidative stress-induced perturbation of mitochondrial membrane potential (Figure 4Cii; n = 3; $^{**}p < 0.01$).

hucMSC-Ex Induces ERK1/2 Phosphorylation and Bcl2 Expression and Inhibits the IKKB/NFkB/casp9/3 Pathway

ERK1/2 MAPK and Bcl2 mediate protection against apoptosis,[25,26] and we noted that hucMSC-Ex induced ERK1/2 phosphorylation and Bcl2 expression at 12 and 24 hr after treatment with hucMSC-Ex in H_2O_2- or CCl_4-injured L02 cells (Figure 5A). Oxidative stress-induced apoptosis is usually associated with caspase activation.[27] Thus, we measured the effect of hucMSC-Ex on the IKKB/NFkB/casp-9/-3 signaling pathway and noted that IKKB and NFkB phosphorylation was inhibited at 24 hr after hucMSC-Ex treatment (Figure 5A). Casp-9 and Casp-3 expression decreased after hucMSC-Ex treatment. hucMSC-Ex dose-dependently inhibited the IKKB/NFkB/casp-9/-3 signaling pathway and pNFkB nuclear translocation and induced Bcl2 expression and ERK1/2 phosphorylation in CCl_4-injured L02 cells (Figures 5B and S5). Compared with recovery by z-vad-FMK, a Road caspase inhibitor, hucMSC-Ex was more effective (Figure 5C). Furthermore, casp-3 activity was dose-dependently inhibited (Figure 5D; n = 3; $^{*}p < 0.05$, $^{**}p < 0.01$). Cleaved casp-3 expression in CCl_4-injured L02 cells (Figure 5Ei) and livers were inhibited (Figure 5Eii). Therefore, hucMSC-Ex induces ERK1/2 phosphorylation and Bcl2 expression and reverses oxidative stress-induced apoptosis.

hucMSC-Ex-Delivered GPX1 Protects Hepatocytes from Oxidative Stress In Vitro and In Vivo

To understand which hucMSC-Ex component offered antioxidant effects, we measured GPX1 and superoxide dismutase (SOD) in L02 cells after exposure to CCl_4 and hucMSC-Ex treatment. GPX1 increased with hucMSC-Ex treatment, and glutathione-S-transferase (GST) activity was also reduced in the hucMSC-Ex group compared with the PBS group (Figure 6A; n = 3; $^{*}p < 0.05$, $^{**}p < 0.01$, $^{***}p < 0.001$). hucMSC-Ex did not change SOD activity in L02 cells (Figure 6A) and had no effect on *GPX1* mRNA expression in L02 cells (Figure 6B).

GPX1 protein was detected in hucMSCs and hucMSC-Ex, and it was greater in hucMSC-Ex compared with HFL-Ex cells (Figure 6C). To investigate the role of GPX1 in hucMSC-Ex-mediated antioxidant activity, we knocked down GPX1 in hucMSCs with small interfering RNA (siRNA) and noted that GPX1 expression was reduced in GPX1 siRNA transfected hucMSCs and hucMSC-Ex (GPX1-siRNA-Ex) (Figure 6D). Gpx activity promotion by hucMSC-Ex treatment was reversed by GPX1 knockdown (Figure 6E; n = 3; $^{**}p < 0.01$). Less MDA and ROS in hucMSC-Ex-treated L02 cells were also reversed

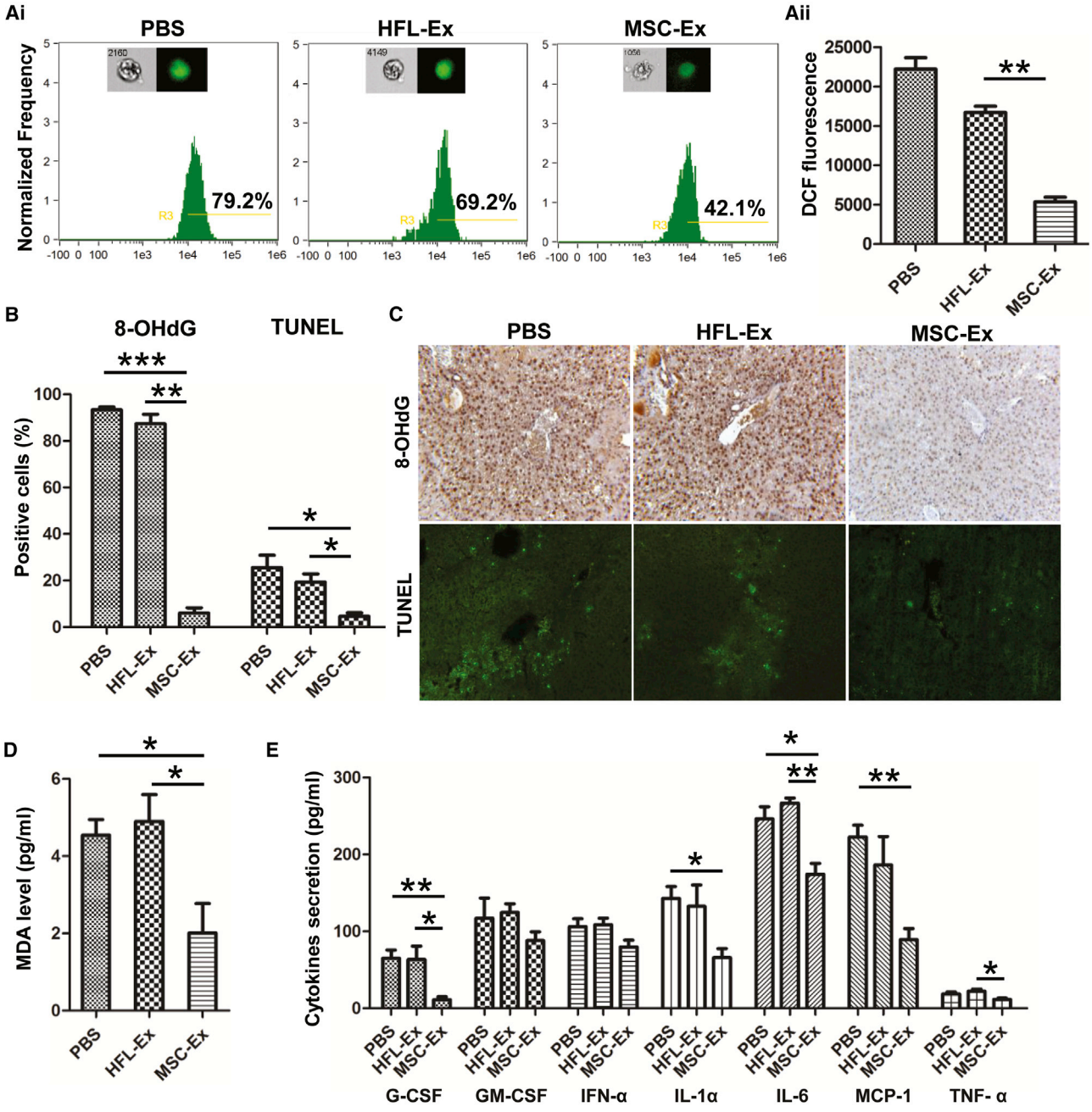

Figure 2. hucMSC-Ex Reduced Oxidative Stress In Vivo

(A) Percentage (Ai) and fluorescence intensity (Aii) of DCF-positive hepatocytes in PBS-, HFL-Ex-, and MSC-Ex-treated livers using imaging flow cytometer. Data show that hucMSC-Ex treatment significantly decreased percentage and fluorescence intensity of DCF-positive hepatocytes. DCF fluorescent values are mean ± SD (n = 4; $^{**}p < 0.01$). (B and C) Immunohistochemical and TUNEL staining of mouse liver slides; reduced oxidative stress marker 8-OHdG expression and apoptosis were found in each group 48 hr after treatment (n = 3; $^{*}p < 0.05$, $^{**}p < 0.01$, $^{***}p < 0.001$). Original magnification 200×. (D) Serum MDA in all groups 48 hr after treatment (n = 3; $^{*}p < 0.05$). (E) Serum G-CSF, GM-CSF, IFN-α, IL-1 α, IL-6, MCP-1, and TNF-α in all groups detected by Luminex assay 48 hr after hucMSC-Ex treatment. hucMSC-Ex treatment reduced pro-inflammatory cytokines (G-CSF, IL-1α, IL-6, MCP-1, and TNF-α) in CCl_4-injured mice (n = 3; $^{*}p < 0.05$, $^{**}p < 0.01$).

by GPX1 knockdown (Figures 6F and 6G; n = 3; $^{*}p < 0.05$, $^{**}p < 0.01$, $^{***}p < 0.001$). hucMSC-Ex-mediated reduction of L02 cell apoptosis, NFkB P65 phosphorylation, and increase of Bcl2 expression were abolished by GPX1 knockdown in vitro (Figures 7A and 7B; n = 3; $^{*}p < 0.05$, $^{**}p < 0.01$). hucMSC-Ex-mediated inhibition of inflammatory infiltration, 8-OHdG expression, and hepatocyte apoptosis was

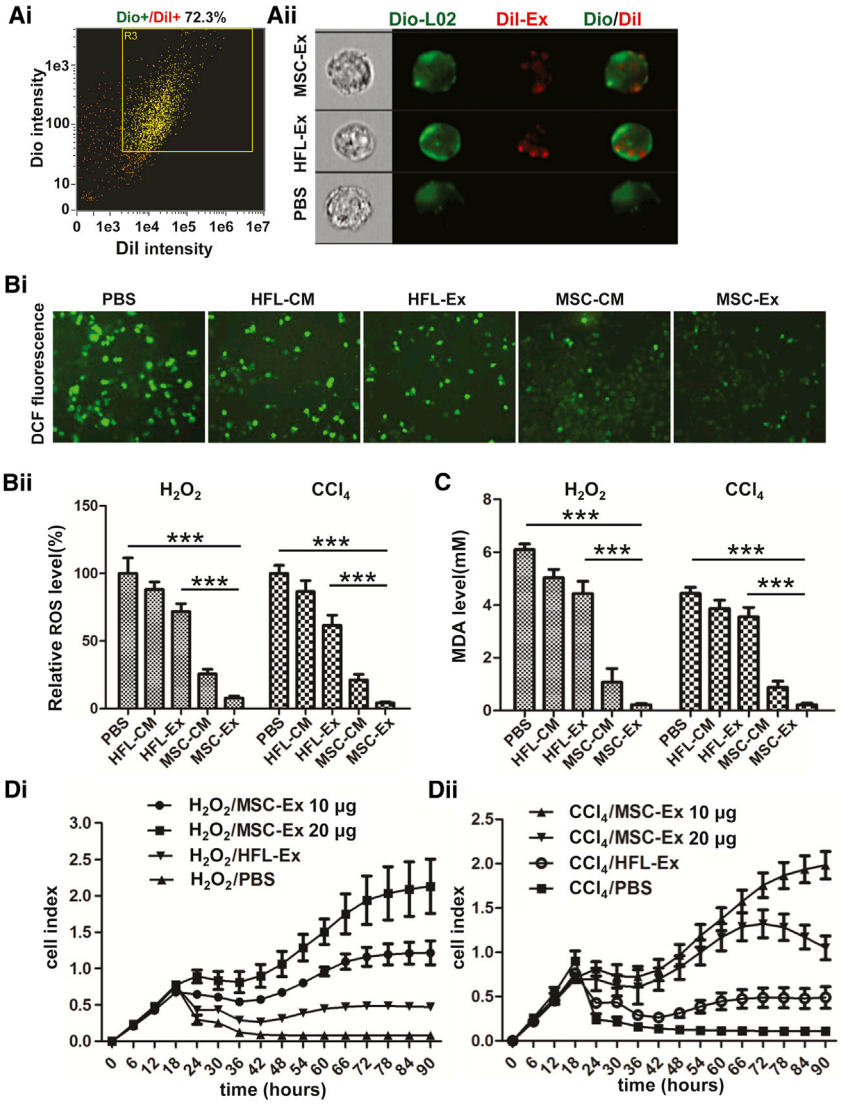

Figure 3. hucMSC-Ex Reduced Oxidative Stress and Increased Cell Viability in LO2 Hepatocytes after CCl_4 and H_2O_2 Treatment

(A) Location of CM-DiI-labeled exosomes (red) in CM-Dio-labeled L02 cells (green) detected by imaging flow cytometry. L02 cells were CM-DiI/CM-Dio positive (i), and CM-DiI-labeled exosomes were found in CM-Dio-labeled L02 cells (ii). (B) ROS production in CCl_4- and H_2O_2-injured L02 cells detected by DCF probe staining after treatment with PBS, HFL-CM, HFL-Ex, MSC-CM, and huMSC-Ex (MSC-Ex). Representative images of DCF fluorescence in CCl_4-injured L02 cells (i) and relative DCF fluorescent values showed reduced ROS production in MSC-Ex treated L02 cells ($n = 5$; $^{***}p < 0.001$) (ii). (C) MDA in CCl_4- and H_2O_2-injured L02 cells treated with PBS, HFL-CM, MSC-CM, or hucMSC-Ex for 24 hr. MDA release was reduced by MSC-Ex treatment ($n = 3$; $^{***}p < 0.001$). (D) L02 cell viability was detected using a real-time cellular analysis system after treatment with CCl_4/PBS, CCl_4/HFL-Ex, or CCl_4/hucMSC-Ex (i) and H_2O_2/PBS, H_2O_2/HFL-Ex, or H_2O_2/hucMSC-Ex (ii) for 90 hr ($n = 3$). L02 cell index was increased by MSC-Ex treatment. Cell sensor impedance is expressed as an arbitrary unit (cell index).

also interfered by GPX1 knockdown in vivo (Figures 7C and 7D; $n = 3$; $^{*}p < 0.05$, $^{**}p < 0.01$). Furthermore, GPX1 knockdown reduced the Gpx activity promotion of ctr-siRNA-Ex in ex vivo hepatocytes ($n = 3$; $^{*}p < 0.05$) (Figure S7A). GPX1 knockdown also attenuated the rescue of hucMSC-Ex on CCl_4-induced liver failure ($n = 10$; $^{*}p < 0.05$) (Figure S7B). Thus, GPX1 knockdown delayed hucMSC-Ex-induced recovery from acute liver injury, so GPX1 is an important factor for hucMSC-Ex-mediated antioxidant activity and liver protection.

DISCUSSION

MSC transplantation has been investigated in clinical trials as potential treatment for liver diseases,[28–30] because systemic injection has been shown to be effective in experimental research.[31–33] This therapeutic effect may include transdifferentiation of MSCs into hepatocyte-like cells, secretion of anti-inflammatory factors, and hepatocyte regeneration promotion at the site of injury.[34–36] Interestingly, Bruno's group confirmed that microvesicles derived from MSCs could protect against acute renal tubular injury via cell-to-cell communication.[37,38] Exosomes/microvesicles contain mRNAs, microRNAs, and proteins, and our previous work indicated that hucMSCs and hucMSC-Ex can alleviate CCl_4-inducued liver injury as that observed in hucMSCs,[10,39] suggesting that MSC-derived exosomes may be critical to reversing liver injury. Thus, we sought to understand the route, dose, and mechanism for the hepatoprotective role of hucMSC-Ex.

Using a murine model of CCl_4-induced acute liver failure, we investigated the route and dose that govern the success and efficacy of using hucMSC-Ex for treatment of liver disease. Our data showed that a single systemic administration of hucMSC-Ex as little as 16 mg/kg body weight effectively rescued the recipient mice from CCl_4-induced liver failure. hucMSC-Ex administrated by the intragastric route have a similar effect as those administered by the tail vein route. hucMSC-Ex administration by the intragastric route may be preferred because it is noninvasive compared with the intrasplenic or intravenous approach commonly used clinically.

We measured the antioxidant activity and the hepatoprotection of hucMSC-Ex. We found that hucMSC-Ex reduced ROS and MDA and increased cell viability in L02 cells exposed to CCl_4 or H_2O_2. Similar data were observed in hucMSC-Ex-treated CCl_4-injured mouse livers. hucMSC-Ex can reverse oxidative stress-induced NFkB apoptosis. Superoxide dismutase (SOD) and glutathione

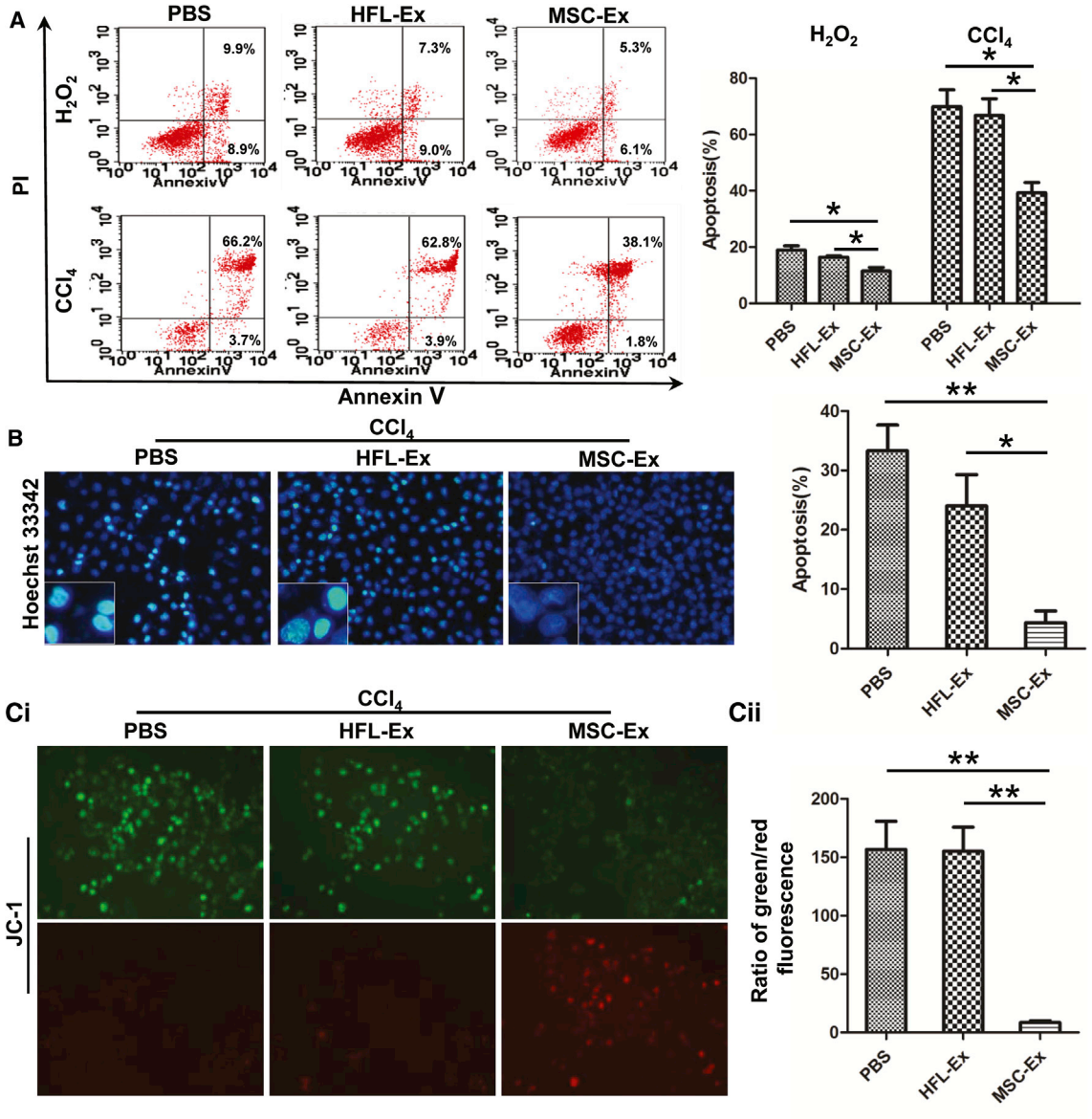

Figure 4. hucMSC-Ex Inhibits Oxidative Stress-Induced Apoptosis In Vitro

(A) Apoptotic L02 cells cultured with PBS, HFL-Ex, or hucMSC-Ex 24 hr after CCl_4 or H_2O_2 treatment visualized with annexin V/PI double staining and flow cytometry. hucMSC-Ex incubation decreased CCl_4- and H_2O_2- induced L02 cell apoptosis compared with PBS and HFL-Ex groups (n = 3; *p < 0.05; **p < 0.01). (B) Hoechst 33342 staining of apoptotic CCl_4- and H_2O_2-injured L02 cells cultured with PBS, HFL-Ex, or hucMSC-Ex for 24 hr. hucMSC-Ex treatment reduced L02 cell apoptosis compared with PBS and HFL-Ex groups (n = 3; *p < 0.05, **p < 0.01). Original magnification 200×. (C) Mitochondrial membrane potentials in PBS, HFL-Ex, and hucMSC-Ex groups. Greater green fluorescence indicates perturbed membrane potentials (n = 3; **p < 0.01). hucMSC-Ex reversed oxidative stress-induced perturbation of mitochondrial membrane potential. Original magnification 200×.

peroxidase 1 (GPX1) are the major endogenous antioxidant enzymes. To understand which exosome component mediated antioxidant effects, SOD and GPX1 were measured in L02 cells after exposure to CCl_4 and hucMSC-Ex treatment. Results showed that GPX1 activity was increased dose-dependently, and SOD activity was not changed in hucMSC-Ex-treated L02 cells. GPX1 is important to hucMSC-Ex-mediated antioxidant and hepatoprotection. Thus, hucMSC-Ex-derived GPX1 was chosen for further analysis.

CCl_4 and H_2O_2 are model hepatotoxicants.[32,40] They were used to develop a mouse liver injury model and study the antioxidant effects of hucMSC-Ex. We measured the levels of ROS, MDA, 8-OHdG, cell viability, and cell apoptosis. Histopathology and

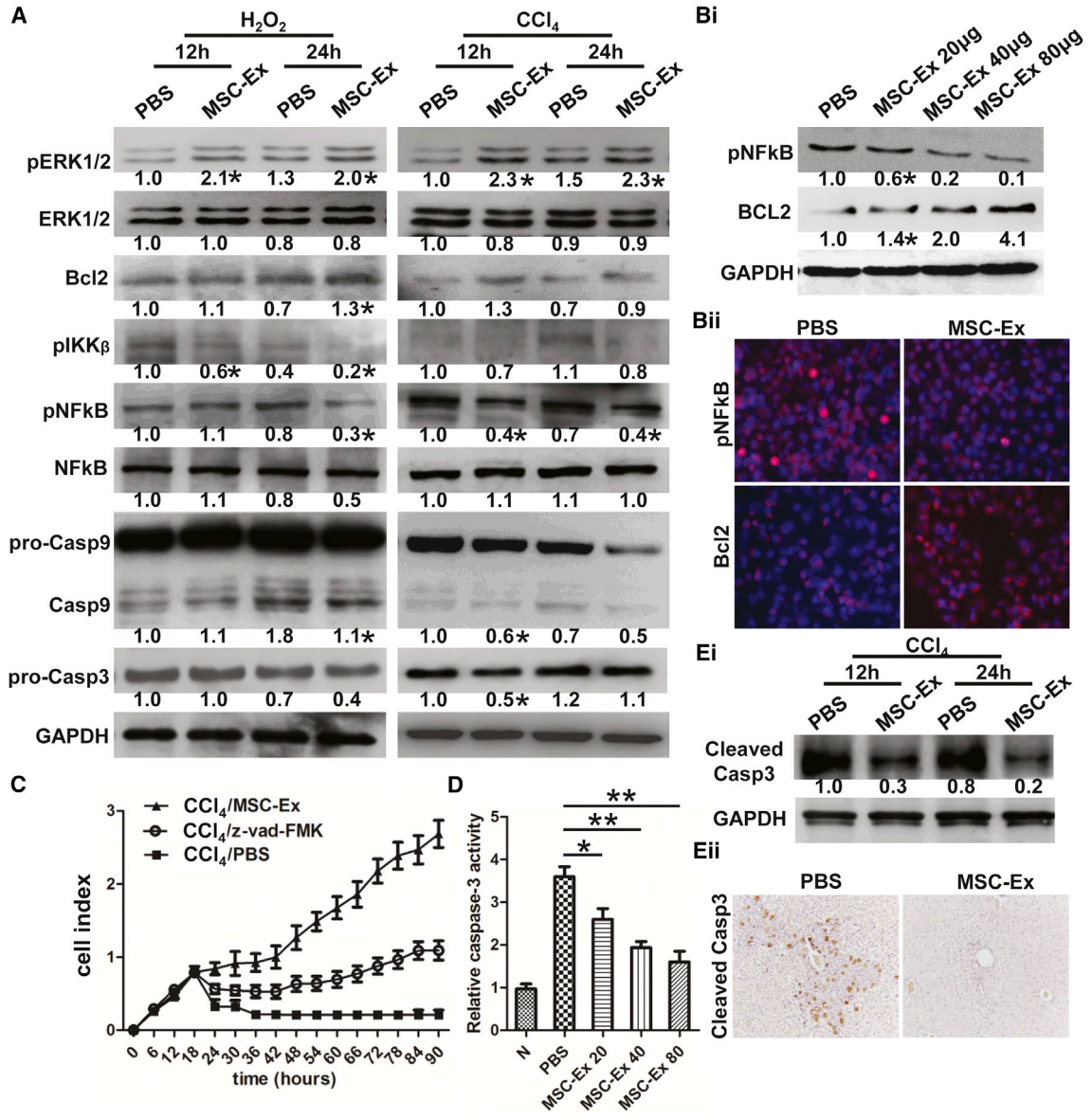

Figure 5. hucMSC-Ex Induces ERK1/2 Phosphorylation and Bcl2 Expression and Inhibits the IKKB/NFkB/Caspase-9/-3 Pathway

(A) Western blot quantification of pERK1/2, total ERK1/2, Bcl2, pIKKβ, pNFkB, total NFkB, and casp9 and casp3. hucMSC-Ex induced ERK1/2 phosphorylation and Bcl2 expression and inhibited IKKB/NFkB/casp-9/-3 signaling in H_2O_2- or CCl_4-injured L02 cells. (B) Bcl2 and pNFkB expression quantified by western blot (i). hucMSC-Ex dose-dependently inhibited pNFkB and induced Bcl2 expression in CCl_4-injured L02 cells. Representative immunofluorescent images of pNFkB and Bcl2 expression in CCl_4-injured L02 cells treated with PBS and hucMSC-Ex (ii). Original magnification 200×. (C) L02 cell viability was recovered by hucMSC-Ex or z-vad-FMK (n = 3). (D) CCl_4-induced casp3 activity was reduced in hucMSC-Ex (20, 40, and 80 μg) (n = 3; *p < 0.05, **p < 0.01). (E) Western blot quantification of cleaved casp3 (i) in CCl_4-injured L02 cells and immunohistochemical staining of cleaved casp3 in CCl_4-injured mouse liver (ii). hucMSC-Ex inhibited cleaved casp3 expression of CCl_4-injured hepatocytes in vitro and in vivo. Original magnification 200×. Data are expressed as relative ratios of specific proteins to GAPDH and shown as numbers under individual blots (n = 3; *p < 0.05).

serum chemistry confirmed that hucMSC-Ex could repair the injured livers. Tetraspanin molecules CD9, CD63, and CD81 are often used to measure exosomes.[41] TEM was used to confirm the size and morphology of exosomes derived from hucMSCs, and western blotting was used to quantify CD9 and CD63 expression in hucMSC-Ex.

Oxidative stress is caused by an imbalance between ROS production and antioxidant defenses that neutralize reactive intermediates, triggering damage. Oxidative stress is associated with liver injury and may arise after CCl_4, H_2O_2, and acetaminophen treatment.[40] We noted that hucMSC-Ex had a significant antioxidant effects in CCl_4- and H_2O_2-injured L02 cells. MDA, ROS, and

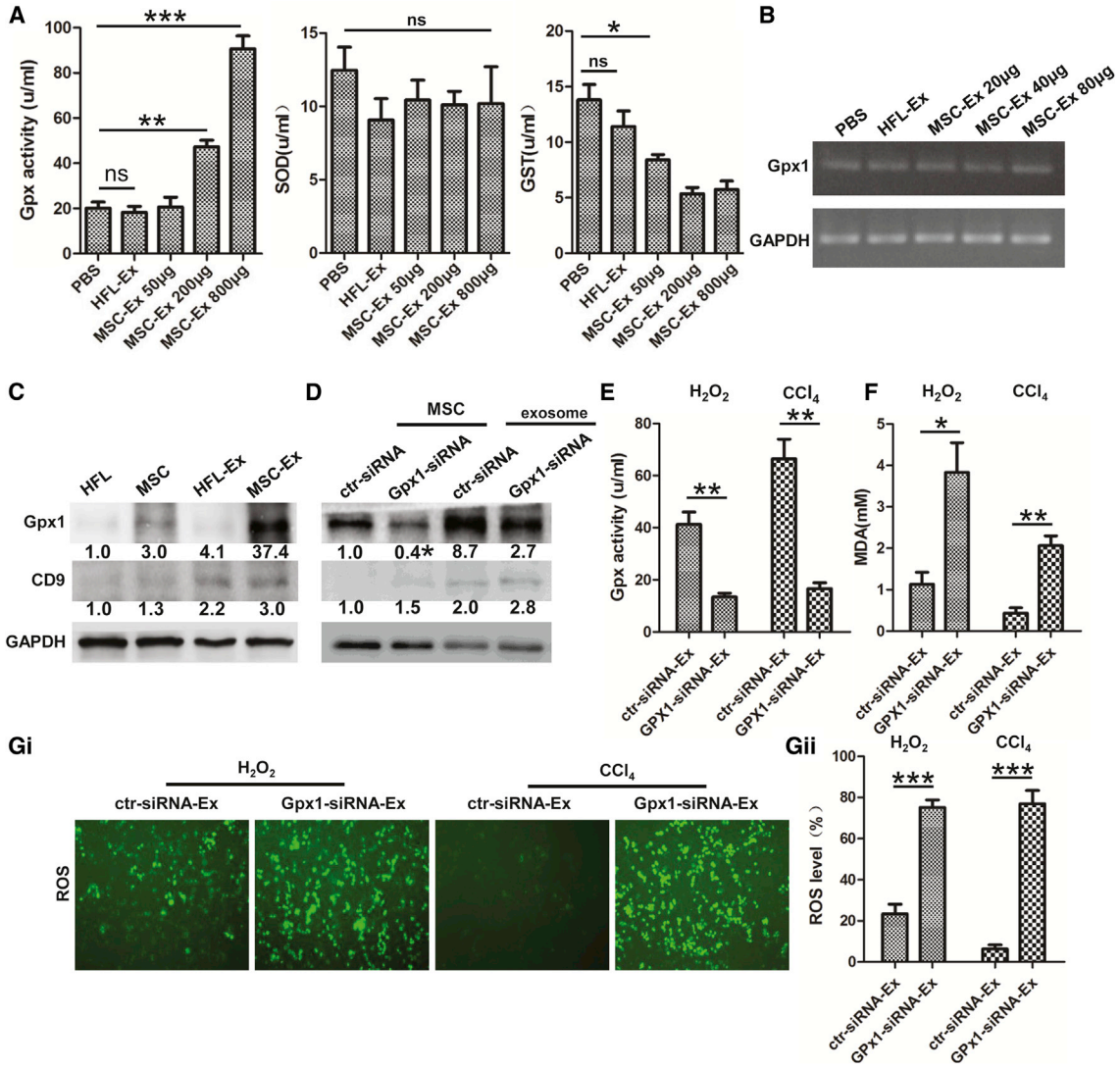

Figure 6. hucMSC-Ex-Delivered GPX1 Protects Hepatocyte from Oxidative Stress In Vitro

(A) CCl_4-injured L02 cells were treated with PBS or hucMSC-Ex (50, 200, and 800 μg) for 24 hr. Intracellular Gpx, SOD, and GST in cell culture were measured, and hucMSC-Ex treatment dose-dependently increased Gpx activity and reduced GST release of L02 cells (n = 3; *p < 0.05, **p < 0.01, ***p < 0.001). (B) Expression of GPX1 mRNA in CCl_4-injured L02 cells was measured with RT-PCR 24 hr after hucMSC-Ex (20, 40, and 80 μg) treatment. GPX1 expression did not change in hucMSC-Ex treated L02 cells. (C) Western blot quantification of GPX1 expression in hucMSCs, HFL, hucMSC-Ex, and HFL-Ex. GPX1 protein was highly expressed in hucMSCs and hucMSC-Ex compared with HFL and HFL-Ex. (D) Western blot quantification of GPX1 expression in GPX1 siRNA transfected hucMSCs and hucMSC-Ex. GPX1 expression was knocked down in hucMSCs and hucMSC-Ex. Data are expressed as relative ratios of specific proteins to GAPDH shown as numbers under individual blots (n = 3; *p < 0.05). (E) After CCl_4- and H_2O_2-injured L02 cells were treated with 300 μg ctr-siRNA and human GPX1-siRNA transfected hucMSC-Ex (ctr-siRNA-Ex and GPX1-siRNA-Ex), Gpx activity of L02 cells was measured 24 hr later. Gpx activity in L02 cells was inhibited in GPX1-siRNA compared with ctr-siRNA-Ex treatment (n = 3; **p < 0.01). (F) MDA measured 24 hr after ctr-siRNA-Ex or GPX1-siRNA-Ex treatment. MDA level was less in ctr-siRNA-Ex treated L02 cells compared with GPX1-siRNA (n = 3; *p < 0.05, **p < 0.01). (G) ROS measurement via DCF in CCl_4- and H_2O_2-injured L02 cells treated with ctr-siRNA-Ex and GPX1-siRNA-Ex for 24 hr (i). ROS were fewer in ctr-siRNA-Ex-treated L02 cells compared with GPX1-siRNA (n = 3; *p < 0.05, **p < 0.01). DCF fluorescent value are mean ± SD (ii) (n = 3; ***p < 0.001). Original magnification 200×.

oxidative stress-induced apoptosis were increased after CCl_4- and H_2O_2-induced injury, which was reduced by hucMSC-Ex treatment. Cell viability significantly increased after hucMSC-Ex treatment. In CCl_4-induced liver injury mouse models, hucMSC-Ex reduced serum MDA, pro-inflammatory cytokine secretion, liver 8-OHdG expression, and cell apoptosis, suggesting the antioxidant activities of hucMSC-Ex.

Recently, Tan's group demonstrated that MSC-Ex is hepatoprotective against CCl_4-induced liver injury via the activation of proliferative

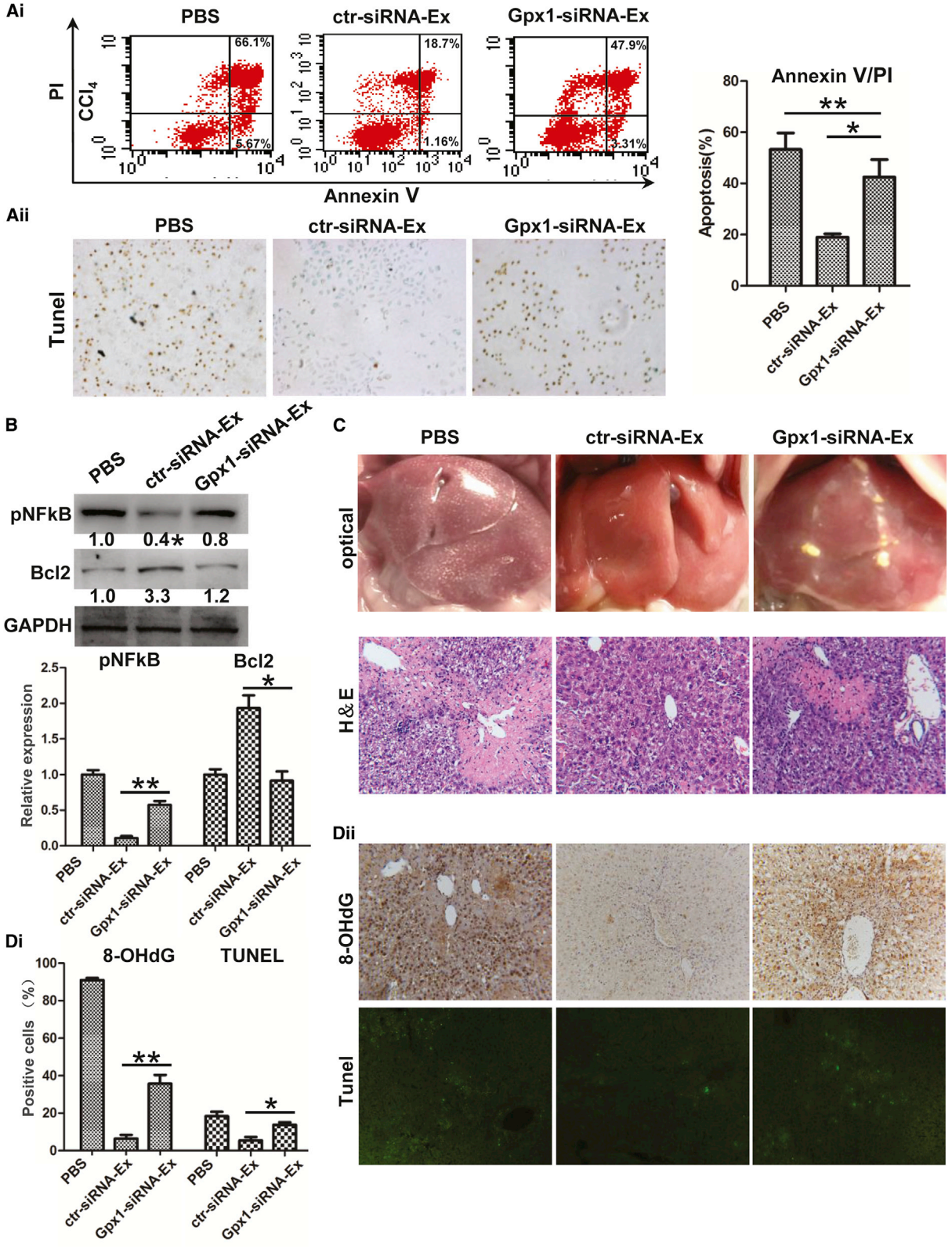

(legend on next page)

and regenerative responses in vitro and in vivo.[42] MSC-Ex had no role in expression of antioxidant genes such as Gpx4, MnSOD, HO-1, and GSR. The role of MSC-Ex administration in hepatic oxidative stress has not been studied. We detected the levels of ROS and other oxidative stress markers to clarify the role of hucMSC-Ex in oxidative stress-induced liver injury. GPX1 gene expression was unchanged after hucMSC-Ex treatment, consistent with previous data. hucMSC-Ex treatment inhibited oxidative stress and increased Gpx activity in L02 cells. Thus, hucMSC-Ex may have antioxidant effects in hepatocytes via Gpx activity modulation but not by regulating antioxidant gene expression.

Exosomes are not only specifically targeted to recipient cells to exchange mRNAs and microRNAs and/or to trigger downstream signaling events, but they also deliver active proteins. MSC-Ex has been shown to promote tissue injury repair via horizontal transfer of mRNAs and microRNAs. Active proteins can be delivered by exosomes to cause biological effects in target cells.[43] We reported a role for exosome-delivered Wnt4 in cutaneous wound healing,[12] but the function of protein molecules transported by MSC-Ex is understudied in liver injury. Evidence indicates that Gpx detoxifies H_2O_2 and is an important antioxidant in humans. Induced GPX1 activity decreases hepatic damage[44,45] and reduces mitochondrial apoptotic pathway activation in cardiomyocytes, chondrocytes, and hepatocytes.[46–48] Our data indicate that abundant GPX1 protein was found in hucMSCs and hucMSC-Ex compared with HFL and HFL-Ex. hucMSC-Ex treatment can protect against changes in the mitochondrial membrane potential and prevent apoptosis by upregulating ERK1/2 phosphorylation and anti-apoptotic Bcl-2 p65 and by inhibiting the IKKB/NFkB/casp-9/-3 signaling pathway. GPX1 knockdown in hucMSCs reduced this antioxidant protection of hucMSC-Ex in vitro, so hucMSCs exosomal GPX1 may be critical for hucMSC-Ex antioxidant-induced recovery from liver injury.

In this study, our results showed that GPX1-containing hucMSC-Ex reduced H_2O_2- and CCl_4-induced L02 cells and liver injury in mice. However, hucMSC-Ex may inhibit H_2O_2- and CCl_4-induced liver injury through different mechanisms. GPX1 could reduce hydrogen peroxide but not phospholipid hydroperoxide. CCl_4 induces the formation of phospholipid peroxides but not hydrogen peroxide. Hepatic GPX1 proteins increased considerably after CCl_4 administration. GPX1 may enhance hepatocytes tolerance to CCl_4-induced oxidative stress through a different mechanism.

In summary, administration of hucMSC-Ex, as little as 16 mg/kg body weight, by either tail vein or oral gavage, engrafted recipient liver, exerted antioxidant and anti-apoptotic effects, and rescued liver failure. hucMSC-Ex offer antioxidant hepatoprotection against CCl_4 and H_2O_2 in vitro and in vivo, and this may be mediated by delivery of GPX1 to reduce hepatic ROS and inhibit oxidative stress-induced apoptosis via upregulation of ERK1/2 and Bcl-2 and downregulation of the IKKB/NFkB/casp-9/-3 pathway. Thus, administration of allogeneic hucMSC-Ex may be an alternative approach for stem cell-based therapy for liver injury and may represent a novel therapeutic strategy for preventing oxidant damage.

MATERIALS AND METHODS

The animal experiments were approved by the ethics committee of Jiangsu University, and the methods were carried out in accordance with the approved guidelines.

Cell Culture

Fresh umbilical cords were collected from informed, consenting mothers at the affiliated Hospital of Jiangsu University. All clinical procedures followed the protocols approved by the ethics committee of Jiangsu University, and the methods were carried out in accordance with the approved guidelines. All participants provided written consent for the present study. hucMSCs were isolated from fresh umbilical cord samples (n = 16) as previously described[39] and maintained in L-DMEM containing 10% fetal bovine serum (FBS) (GIBCO) at 37°C with 5% CO_2. Human lung fibroblasts (HFL-1) were purchased from the Chinese Academy of Sciences and cultured with minimal essential medium alpha (MEM-α) containing 15% FBS (GIBCO) at 37°C with 5% CO_2. Human L02 cells were purchased from the Chinese Academy of Sciences and maintained in RPMI 1640 containing 10% FBS (GIBCO) at 37°C with 5% CO_2. All cells were tested for mycoplasma contamination.

Isolation and Characterization of Exosomes

Exosomes were isolated and purified by ultracentrifugation as previously described.[22] Briefly, bovine exosomes and protein aggregates in DMEM/10% FBS were removed by ultracentrifugation at 100,000 × *g* for 16 hr at 4°C. hucMSCs and HFL-1-conditional medium (MSC-CM and HFL-CM) were collected after 48 hr culture and centrifuged for 20 min at 2,000 × *g* to remove cell debris. Then supernatant was transferred to an ultracentrifuge tube underlain with 30% sucrose/D_2O cushion (density 1.210 g/cm^3), followed by ultracentrifugation at 100,000 × *g* for 1 hr at 4°C. Exosomes were collected from the bottom of the tube and concentrated using 100 KDa molecular weight

Figure 7. GPX1 Knockdown Reduced Antioxidants and Antiapoptosis

(A) Apoptotic CCl_4-injured L02 cells were analyzed by annexin V/PI and TUNEL staining after treated with ctr-siRNA-Ex and GPX1-siRNA-Ex for 24 hr. Percentage of apoptotic L02 cell was lower in the ctr-siRNA-Ex group compared with the GPX1-siRNA-Ex group (n = 3; *p < 0.05, **p < 0.01). (B) Western blot quantification of Bcl2 and pNFkB expression in CCl_4-injured L02 cells 24 hr after PBS, ctr-siRNA-Ex or GPX1-siRNA-Ex treatment. pNFkB inhibition and Bcl2 promotion occurred in the ctr-siRNA-Ex group but not in the GPX1-siRNA-Ex group (n = 3; *p < 0.05, **p < 0.01). (C) Representative optical and H&E images of mouse livers 48 hr after PBS, ctr-siRNA-Ex, or GPX1-siRNA-Ex treatment. Inflammatory infiltration was reduced by ctr-siRNA-Ex treatment compared with GPX1-siRNA-Ex treatment. Original magnification 200×. (D) 8-OHdG and TUNEL staining in CCl_4-injured mouse livers 48h after PBS, ctr-siRNA-Ex, or GPX1-siRNA-Ex treatment. 8-OHdG expression and apoptosis were reduced by ctr-siRNA-Ex compared with GPX1-siRNA-Ex treatment. Original magnification 200× (n = 3; *p < 0.05, **p < 0.01).

cutoff ultrafiltration membrane (MWCO) (Millipore) at 1,000 × *g* for 30 min. Purified exosomes in supernatant were subjected to filtration on a 0.22-μm-pore filter (Millipore). The final pellet (hucMSC-Ex and HFL-Ex) was resuspended in 100 μL PBS and stored at −80°C. The protein content of the concentrated exosomes was determined using BCA protein assay kit (Pierce, ThermoFisher). Morphology of the exosomes was observed using transmission electron microscopy (FEI Tecnai 12, Philips). The size and relative intensity of exosomes were detected by nanoparticle tracking analysis (NTA) using NanoSight instruments.

Acute Liver Injury Mice Model and Exosome Injection

All experimental procedures were in accordance with Chinese legislation regarding experimental animals. BALB/c-nu/nu female mice aged 4–5 weeks were purchased from the Laboratory Animal Center, Yangzhou University. Carbon tetrachloride (CCl_4) was dissolved in mineral oil at 10% concentration and administered to animals by gavage. Doses between 0.15 and 0.35 mL CCl_4/kg body weight were tested for hepatotoxicity and lethality by intraperitoneal injection. At 24 hr post-CCl_4 injection, mice were randomized into six groups: PBS group, mice injected with 1 mL PBS (n = 20); HFL-Ex group, mice injected with HFL-Ex by tail vein (n = 20); and hucMSC-Ex 8mg/kg body weight (n = 20), 16 mg/kg body weight (n = 20), 32 mg/kg body weight groups (n = 20), mice treated with hucMSC-Ex by tail vein or intragastric administration. The final concentration of exosomes used for treating liver injury was 20 mg/ml to treat each animal. At days 1, 3, 5, and 7 post-exosome injection, blood samples were collected and entire livers were taken and prepared for further analysis from sacrificed mice.

Exosome Labeling and Tracking in L02 Cells and Mice

Exosomes and L02 cells were labeled with CM-Dil and CM-Dio (Molecular Probes, ThermoFisher) separately according to the manufacturer's protocol. Exosomes (20 μg) and L02 cells (1×10^5 cells) in suspension were mixed with CM-Dil and CM-Dio in the dark at 37°C for 30 min separately. CM-Dil-labeled exosomes were washed with PBS and concentrated with a 100 KDa molecular weight cutoff ultrafiltration membrane (MWCO) (Millipore) at 1,000 × *g* for 30 min. CM-Dio-labeled L02 cells were centrifuged at 800 × *g* for 5 min to remove non-binding dye. Then CM-Dil-labeled exosomes were incubated with CM-Dio-labeled L02 cells at 37°C for 24 hr. After incubation, fluorescent intensity of incubated cells was assayed with an ImageStreamX Imaging Flow Cytometer (Amnis) at 60× magnification and a minimum of 10,000 cells for all samples. Bright-field and fluorescent images were collected using IDEAS software (Amnis). For the distribution of CM-Dil-labeled exosomes in cultured L02 cells, CM-Dil-labeled exosomes were incubated with L02 cells at 37°C for 24 hr and detected by fluorescent images.

For the distribution of exosomes in CCl_4-injured mice, CM-Dir-labeled (Ruitaibio) exosomes injected into CCl_4-injured and normal mice were imaged using a Maestro In Vivo Imaging System (CRI). Scans were performed 24 hr after exosome injection (20 mg) via the tail vein at 630 nm (λex). In vivo spectral imaging from 690–850 nm was performed using an exposure time of 150 ms per image frame. Autofluorescence was removed with spectral unmixing software.

ALT, AST, and GST Assay

Serum AST and alanine aminotransferase (ALT) levels were measured using an automated biochemical analyzer (n = 5). A commercial kit was used to quantify the level of glutathione-S-transferase (GST) according to the protocol (n = 3) (Beyotime).

Histopathological Staining

Liver tissues were processed for paraffin embedding and were sectioned into 4 mm sections. The sections were stained with hematoxylin and eosin (H&E) staining and Masson's trichrome (MT) staining according to standard protocols (Yuanye Biology). To analyze the extent of liver fibrosis, randomly picked fields of MT sections were captured from each animal.

Immunohistochemistry and Immunocytochemistry

Mouse liver slides were fixed in 4% formaldehyde solution at room temperature overnight. These liver slides were incubated with CD63 (Bioworld) and 8-OHdG antibodies (Japan Institute for Control of Aging) according to the manufacturer's instructions. The signals were visualized with 3,30-dimino benzidine (Boster) and counterstained with hematoxylin. The morphological sections were evaluated by high-power light microscopy examination (Nikon). In vitro, the L02 cells were fixed in 4% paraformaldehyde for 10 min. To examine Bcl2 and pNFkB expression, L02 cells were incubated with anti-Bcl2 (Bioworld) and pNFkB (SAB) and fluorescent-labeled secondary antibody. Then slides were counterstained with DAPI and examined under a fluorescent microscope. Fluorescence imaging was performed with an Olympus Fluorescence Microscope (magnification 200×).

TUNEL Assay

Cell apoptosis in liver slides and CCl_4-injured L02 were measured using an in situ cell apoptosis kit (Vazyme Biotechnology) and the FragEL DNA Fragmentation Detection Kit (Merk Millipore), respectively, according to the manufacturer's instructions.

Luminex Assay

Serum levels of granulocyte colony-stimulating factor (G-CSF), granulocyte-macrophage colony-stimulating factor (GM-CSF), interferon-α (IFN-α), interleukin (IL)-1α, IL-6, monocyte chemoattractant protein-1 (MCP-1), and tumor necrosis factor-α (TNF-α) in exosomes treated mice livers were measured using Luminex kits in accordance with the manufacturer's instructions (Millipore).

CCl_4- and H_2O_2-Induced L02 Cell Injury In Vitro

L02 cells were seeded in six-well plates (1×10^5 cells/well), and at ~70% confluence, cells were treated with medium containing 0.1 mM CCl_4/exosomes or 400 μM H_2O_2/exosomes for 12 or 24 hr. PBS or HFL-CM, HFL-Ex, and MSC-CM were controls (final concentration of exosomes 20 mg/ml; various concentrations including 10,

20, 40, and 80 μg were used) were applied to L02. After exosome treatment, cells were collected and lipid peroxidation and RNA and protein were measured or samples were fixed in 4% paraformaldehyde for histology.

ROS Measurement

Production of tissue and cellular ROS was measured with a nonfluorescent cell-permeating compound, 2′-7′-dichlorofluorescein diacetate (DCF-DA) (Beyotime). DCF-DA is hydrolyzed by intracellular esterases and oxidized by ROS to a fluorescent compound, DCF. For the ROS of liver tissues, the hepatocytes were isolated with homogenate method and incubated with DCF-DA (10 μM) for 30 min at 37°C. After washing with PBS, DCF-positive cells and intracellular fluorescence intensity were detected with ImageStreamX Imaging Flow Cytometer at 60× magnification and a minimum of 10,000 cells for all samples. Bright-field and fluorescent images were collected using IDEAS software. Similarly, hucMSC-Ex-treated L02 cells were incubated with DCF-DA (10 μM) for 30 min at 37°C. Intracellular fluorescence was observed with Olympus Fluorescent Microscope (200×) and quantified by fluorescent intensity with Image-Pro Plus 6.0 software.

Lipid Peroxidation Assay

Malondialdehyde (MDA) was measured according to the manufacturer's protocol (Beyotime). L02 cells were harvested by trypsinization, and cell extracts were prepared by sonication in ice cold buffer (50 mM Tris-HCl [pH 7.5], 5 mM EDTA, and 1 mM DTT). Lysed cells were centrifuged at 10,000 × *g* for 20 min to remove debris. The supernatant was subjected to the measurement of MDA level and the protein contents. A BCA assay kit (Pierce) was used to quantify protein concentration. MDA level was then normalized to milligrams of protein. Three experiments were performed.

Cell Viability by Real-Time Cellular Analysis

Cell viability of exosome-treated L02 was measured using a real-time cellular analysis (RTCA) system according to the manufacturer's instruction (xCELLigence). Cell viability was monitored continuously after applying increased concentrations of exosome protein. Briefly, background measurements were taken after adding 100 μL PBS to the wells. Next, cells were seeded at a density of 5,000 cells/well on a 96-well plate with electrodes for 18 hr to allow cells to grow to the log phase. Cells were treated with CCl_4 (0.1 mM)/exosome or H_2O_2 (400 μM)/exosome dissolved in cell culture media and continuously monitored for up to 90 hr. Different dose of exosomes (10 μg, 20 μg) were applied to treat L02 cells. Cell sensor impedance was expressed as an arbitrary unit called the cell index and recorded every 5 min by RTCA. Three experiments were performed.

Hoechst 33342 Staining and Annexin V/PI Double Staining

CCl_4- and H_2O_2-treated L02 cells were incubated with PBS or exosomes for 24 hr. Then the cells were incubated in PBS containing 50 μg/mL of Hoechst 33342 (Sigma-Aldrich) at 37°C for 20 min. After washing with PBS, cells were examined under an Olympus Fluorescence Microscope (magnification 200×). Apoptotic cells were identified by the typical morphology, including shrinkage of the cytoplasm, membrane blebbing, and nuclear condensation and/or fragmentation. For quantification of apoptosis, L02 cells were treated as described above. The cells were harvested and subjected to annexin V/PI double staining (Invitrogen) and analyzed by fluorescence-activated cell sorting (FACS) using a flow cytometer (FACS Calibur, BD). Briefly, both floating and attached cells were pooled, washed, and resuspended in the annexin V binding buffer. Alexa Fluor 488 annexin V and PI were added to suspended cells, and the reaction was incubated in the dark for 10 min. Flow cytometric analysis was performed by analyzing gated cells. All experiments were performed at least three times.

Mitochondrial Membrane Potential Assay

Mitochondrial membrane potential was measured using JC-1 staining according to the manufacturer's instruction (Beyotime). L02 cells were treated with CCl_4/exosomes in six-well plates as described above. Then medium were changed with 1 mL fresh medium containing JC-1 (5 μg/mL) and incubated at 37°C for 20 min. After washing twice with JC-1 staining solution (1 μg/mL), images were obtained by fluorescent microscopy and analyzed for green and red fluorescence using Image-Pro Plus 6.0 software. Mitochondrial membrane potential depolarization was expressed by an increase in the green/red fluorescent intensity ratio (n = 3).

Caspase-3 Activity Assay

The activity of caspase-3 was determined using a caspase-3 activity kit (Beyotime). Cell lysates were prepared after exosome treatment. Assays were performed on 96-well microtiter plates by incubating 10 μL protein of cell lysate per sample in 80 μL reaction buffer (1% NP-40, 20 mM Tris-HCl [pH 7.5], 137 mM Nad, and 10% glycerol) containing 10 μL caspase-3 substrate (Ac-DEVD-pNA) (2 mM). Lysates were incubated at 37°C for 4 hr. Samples were measured at wavelengths of 405 nm according to the manufacturer's protocol.

Cellular Glutathione Peroxidase and Superoxide Dismutase Activity

For the glutathione peroxidase (Gpx) activity of L02 cells, L02 cells were treated with CCl_4/exosomes as described above, and activity of Gpx was determined after 24 hr. Cell extracts were prepared using cell lysis buffer (20 mmol/L Tris, 150 mmol/L NaCl, 1% Triton X-100, 5 mmol/L sodium pyrophosphate) and were centrifuged at 12,000 × *g* for 10 min at 4°C. For the Gpx activity of exosomes, 60 μg exosomes were lysed using the above cell lysis buffer and centrifuged at 12,000 × *g* for 10 min at 4°C. Gpx activity (nmol NADPH/min/mL) was measured in the supernatant using a cellular glutathione peroxidase assay kit that measures the coupled oxidation of NADPH during glutathione reductase (GR) recycling of oxidized glutathione from Gpx-mediated reduction of t-butyl peroxide (Beyotime). In the assay, excess GR, glutathione, and NADPH were added according to the manufacturer's instructions. Gpx activity results of L02 cells and exosomes were expressed as u/ml and u/mg, respectively. For the assay of superoxide dismutase (SOD) activity,

Table 1. Primers for RT-PCR and Real-Time PCR

Genes	Primer Sequence (5′-3′)	Annealing Temperature (°C)	Product Size (bp)
Human GPX1	for: TATCGAGAATGTGGCGTCCC	60	143
	rev: TCTTGGCGTTCTCCTGATGC		
β-actin	for: CACGAAACTACCTTCAACTCC	58	265
	rev: CATACTCCTGCTTGCTGATC		
GAPDH	for: GGATTTGGTCGTATTGGG	55	205
	rev: GGAAGATGGTGATGGGATT		

for, forward; rev, reverse.

CCl_4/exosome-treated L02 cells were centrifuged at 1,000 × *g* for 5 min and washed with cold PBS. Then the cell pellets were lysed using homogenizer and centrifuged at 12,000 × *g* for 10 min at 4°C. SOD activity was measured in the supernatant using the Total Superoxide Dismutase Assay Kit according to the manufacturer's instruction (Beyotime). Three experiments were performed.

Transient Transfection of Plasmids and siRNAs

For hucMSCs cell transfection, Lipofectamine 2000 reagent (Life Technologies) was used to transfect human GPX1 siRNA and control siRNA oligos (Santa Cruz Biotechnology) according to the manufacturer's instructions. Transfected cells were cultured for exosome extraction or processed for western blot analysis at 48 hr after transfection. The exosomes derived from GPX1 siRNA-treated and control siRNA-treated hucMSCs were identified as ctr-siRNA-Ex and GPX1-siRNA-Ex. The protein content of the extracted exosomes was determined using a BCA protein assay kit. Three experiments were performed. For the survival of ctr-siRNA-Ex-treated and GPX1-siRNA-Ex-treated mice, mice were randomized into three groups: PBS group, mice injected with 1 mL PBS (n = 10); ctr-siRNA-Ex 32 mg/kg body weight group (n = 10), mice injected with ctr-siRNA-Ex by tail vein; and GPX1-siRNA-Ex 32 mg/kg body weight group (n = 10), mice treated with GPX1-siRNA-Ex by tail vein or intragastric administration.

Western Blot

Cells were harvested and lysed in RIPA buffer. Protein concentration was determined using the BCA assay kit. Equal amounts of cell lysates were loaded and separated on a 12% SDS-PAGE gel. Transferred membranes were incubated with the primary antibodies against Bcl2 (Bioworld), CD9 (Bioworld), CD61 (Bioworld), CD63 (Bioworld), pERK1/2 (Santa Cruz), ERK1/2 (Santa Cruz), pIKKβ (SAB), pNFkB (SAB), NFkB (SAB), Casp9 (Santa Cruz), Casp3 (Santa Cruz), cleaved Casp3 (Santa Cruz), and GAPDH (KangCheng) overnight at 4°C. After incubation and washing with TBST (tris-buffered saline with 0.05% Tween-20), membranes were challenged with HRP-conjugated goat anti-rabbit or goat anti-mouse antibodies (dilution 1:2,000), followed by an enhanced chemiluminescent substrate (ECL). The signals were visualized by using Luminata crescendo western horseradish peroxidase (HRP) substrate (Millipore).

RT-PCR

Total RNA of L02 cells was extracted with the Trizol reagent and a DNase (Invitrogen) treatment to remove any genomic DNA. cDNA was synthesized using oligo dT primers with SuperScriptTM II RT kit according to the manufacturer's instructions (Invitrogen). Primers to generate specific products were designed as shown in Table 1. Primers were produced by Shanghai Bio-Engineering. PCRs were carried out in a PCR thermal cycler (PCR Express, Thermo Hybaid).

Statistical Analysis

Data are expressed as mean ± SD. Statistical significance was determined by Student's t test (two-tailed) using Prism software (GraphPad). Animal survival was analyzed by log rank tests, and p values are as shown. All significance was defined at the $p < 0.05$ level.

SUPPLEMENTAL INFORMATION

Supplemental Information includes seven figures and can be found with this article online at http://dx.doi.org/10.1016/j.ymthe.2016.11.019.

AUTHOR CONTRIBUTIONS

W.X., Y.Y., and H.Q. conceived experiments, analyzed results, and wrote the manuscript. W.X., Y.Y., and F.M. secured funding. Y.Y., W.J., Y.T., S.Z., F.M., and A.G. performed experiments. Y.Y and H.Z. provided reagents, expertise, and feedback.

CONFLICTS OF INTEREST

The authors declare no conflicts of interest.

ACKNOWLEDGMENTS

This work was funded by the National Natural Science Foundation of China (81200312, 81670549, and 81670502), the China Postdoctoral Science Foundation (2015M580403 and 2016T90431), the Natural Science Foundation of Jiangsu Province (BE2016717 and BK2012288), the Scientific Research Foundation of Jiangsu University (11JDG062), Priority Academic Program Development of Jiangsu Higher Education Institutions (PAPD), and the Young Backbone Teacher Training Project of Jiangsu University.

REFERENCES

1. Fisher, K., Vuppalanchi, R., and Saxena, R. (2015). Drug-induced liver injury. Arch. Pathol. Lab. Med. *139*, 876–887.

2. Phinney, D.G., and Prockop, D.J. (2007). Concise review: mesenchymal stem/multipotent stromal cells: the state of transdifferentiation and modes of tissue repair—current views. Stem Cells *25*, 2896–2902.

3. Kolf, C.M., Cho, E., and Tuan, R.S. (2007). Mesenchymal stromal cells. Biology of adult mesenchymal stem cells: regulation of niche, self-renewal and differentiation. Arthritis Res. Ther. *9*, 204.

4. Stoltz, J.F., de Isla, N., Li, Y.P., Bensoussan, D., Zhang, L., Huselstein, C., Chen, Y., Decot, V., Magdalou, J., Li, N., et al. (2015). Stem cells and regenerative medicine: myth or reality of the 21th century. Stem Cells Int. *2015*, 734731.

5. Xu, X., Qian, H., Zhu, W., Zhang, X., Yan, Y., Wang, M., and Xu, W. (2010). Isolation of cancer stem cells from transformed human mesenchymal stem cell line F6. J. Mol. Med. (Berl.) *88*, 1181–1190.

6. Kuo, T.K., Hung, S.P., Chuang, C.H., Chen, C.T., Shih, Y.R., Fang, S.C., et al. (2008). Stem cell therapy for liver disease: parameters governing the success of using bone marrow mesenchymal stem cells. Gastroenterology *134*, 2111–2121.
7. Xin, H., Li, Y., Buller, B., Katakowski, M., Zhang, Y., Wang, X., Shang, X., Zhang, Z.G., and Chopp, M. (2012). Exosome-mediated transfer of miR-133b from multipotent mesenchymal stromal cells to neural cells contributes to neurite outgrowth. Stem Cells *30*, 1556–1564.
8. Hu, G.W., Li, Q., Niu, X., Hu, B., Liu, J., Zhou, S.M., Guo, S.C., Lang, H.L., Zhang, C.Q., Wang, Y., and Deng, Z.F. (2015). Exosomes secreted by human-induced pluripotent stem cell-derived mesenchymal stem cells attenuate limb ischemia by promoting angiogenesis in mice. Stem Cell Res. Ther. *6*, 10.
9. Nakamura, Y., Miyaki, S., Ishitobi, H., Matsuyama, S., Nakasa, T., Kamei, N., Akimoto, T., Higashi, Y., and Ochi, M. (2015). Mesenchymal-stem-cell-derived exosomes accelerate skeletal muscle regeneration. FEBS Lett. *589*, 1257–1265.
10. Li, T., Yan, Y., Wang, B., Qian, H., Zhang, X., Shen, L., Wang, M., Zhou, Y., Zhu, W., Li, W., and Xu, W. (2013). Exosomes derived from human umbilical cord mesenchymal stem cells alleviate liver fibrosis. Stem Cells Dev. *22*, 845–854.
11. Zhou, Y., Xu, H., Xu, W., Wang, B., Wu, H., Tao, Y., Zhang, B., Wang, M., Mao, F., Yan, Y., et al. (2013). Exosomes released by human umbilical cord mesenchymal stem cells protect against cisplatin-induced renal oxidative stress and apoptosis in vivo and in vitro. Stem Cell Res. Ther. *4*, 34.
12. Zhang, B., Wang, M., Gong, A., Zhang, X., Wu, X., Zhu, Y., Shi, H., Wu, L., Zhu, W., Qian, H., and Xu, W. (2015). HucMSC-Exosome Mediated-Wnt4 Signaling Is Required for Cutaneous Wound Healing. Stem Cells *33*, 2158–2168.
13. Lai, R.C., Chen, T.S., and Lim, S.K. (2011). Mesenchymal stem cell exosome: a novel stem cell-based therapy for cardiovascular disease. Regen. Med. *6*, 481–492.
14. Valadi, H., Ekström, K., Bossios, A., Sjöstrand, M., Lee, J.J., and Lötvall, J.O. (2007). Exosome-mediated transfer of mRNAs and microRNAs is a novel mechanism of genetic exchange between cells. Nat. Cell Biol. *9*, 654–659.
15. Ivanov, A.V., Smirnova, O.A., Petrushanko, I.Y., Ivanova, O.N., Karpenko, I.L., Alekseeva, E., Sominskaya, I., Makarov, A.A., Bartosch, B., Kochetkov, S.N., and Isaguliants, M.G. (2015). HCV core protein uses multiple mechanisms to induce oxidative stress in human hepatoma Huh7 cells. Viruses *7*, 2745–2770.
16. Li, H., Zhu, W., Zhang, L., Lei, H., Wu, X., Guo, L., Chen, X., Wang, Y., and Tang, H. (2015). The metabolic responses to hepatitis B virus infection shed new light on pathogenesis and targets for treatment. Sci. Rep. *5*, 8421.
17. Yu, Y., Guerrero, C.R., Liu, S., Amato, N.J., Sharma, Y., Gupta, S., et al. (2015). Comprehensive assessment of oxidatively induced modifications of DNA in a rat model of human Wilson's disease. Mol. Cell. Proteomics *15*, 810–817.
18. Gentric, G., Maillet, V., Paradis, V., Couton, D., L'Hermitte, A., Panasyuk, G., Fromenty, B., Celton-Morizur, S., and Desdouets, C. (2015). Oxidative stress promotes pathologic polyploidization in nonalcoholic fatty liver disease. J. Clin. Invest. *125*, 981–992.
19. Takaki, A., and Yamamoto, K. (2015). Control of oxidative stress in hepatocellular carcinoma: Helpful or harmful? World J. Hepatol. *7*, 968–979.
20. Singal, A.K., Jampana, S.C., and Weinman, S.A. (2011). Antioxidants as therapeutic agents for liver disease. Liver Int. *31*, 1432–1448.
21. Brigelius-Flohé, R., and Maiorino, M. (2013). Glutathione peroxidases. Biochim. Biophys. Acta *1830*, 3289–3303.
22. Zhu, W., Huang, L., Li, Y., Zhang, X., Gu, J., Yan, Y., Xu, X., Wang, M., Qian, H., and Xu, W. (2012). Exosomes derived from human bone marrow mesenchymal stem cells promote tumor growth in vivo. Cancer Lett. *315*, 28–37.
23. Hafez, M.M., Al-Shabanah, O.A., Al-Harbi, N.O., Al-Harbi, M.M., Al-Rejaie, S.S., Alsurayea, S.M., and Sayed-Ahmed, M.M. (2014). Association between paraoxonases gene expression and oxidative stress in hepatotoxicity induced by CCl4. Oxid. Med. Cell. Longev. *2014*, 893212.
24. Wang, K. (2014). Molecular mechanisms of hepatic apoptosis. Cell Death Dis. *5*, e996.
25. Guégan, J.P., Frémin, C., and Baffet, G. (2012). The MAPK MEK1/2-ERK1/2 pathway and its implication in hepatocyte cell cycle control. Int. J. Hepatol. *2012*, 328372.
26. Lei, K., Nimnual, A., Zong, W.X., Kennedy, N.J., Flavell, R.A., Thompson, C.B., Bar-Sagi, D., and Davis, R.J. (2002). The Bax subfamily of Bcl2-related proteins is essential for apoptotic signal transduction by c-Jun NH(2)-terminal kinase. Mol. Cell. Biol. *22*, 4929–4942.
27. Riedl, S.J., and Shi, Y. (2004). Molecular mechanisms of caspase regulation during apoptosis. Nat. Rev. Mol. Cell Biol. *5*, 897–907.
28. Meier, R.P., Müller, Y.D., Morel, P., Gonelle-Gispert, C., and Bühler, L.H. (2013). Transplantation of mesenchymal stem cells for the treatment of liver diseases, is there enough evidence? Stem Cell Res. (Amst.) *11*, 1348–1364.
29. Houlihan, D.D., Hopkins, L.J., Suresh, S.X., Armstrong, M.J., and Newsome, P.N. (2011). Autologous bone marrow mesenchymal stem cell transplantation in liver failure patients caused by hepatitis B: short-term and long-term outcomes. Hepatology *54*, 1891–1892.
30. Zhang, Z., Lin, H., Shi, M., Xu, R., Fu, J., Lv, J., Chen, L., Lv, S., Li, Y., Yu, S., et al. (2012). Human umbilical cord mesenchymal stem cells improve liver function and ascites in decompensated liver cirrhosis patients. J. Gastroenterol. Hepatol. *27* (*Suppl 2*), 112–120.
31. van Poll, D., Parekkadan, B., Cho, C.H., Berthiaume, F., Nahmias, Y., Tilles, A.W., and Yarmush, M.L. (2008). Mesenchymal stem cell-derived molecules directly modulate hepatocellular death and regeneration in vitro and in vivo. Hepatology *47*, 1634–1643.
32. Meier, R.P., Mahou, R., Morel, P., Meyer, J., Montanari, E., Muller, Y.D., Christofilopoulos, P., Wandrey, C., Gonelle-Gispert, C., and Bühler, L.H. (2015). Microencapsulated human mesenchymal stem cells decrease liver fibrosis in mice. J. Hepatol. *62*, 634–641.
33. Park, M., Kim, Y.H., Woo, S.Y., Lee, H.J., Yu, Y., Kim, H.S., Park, Y.S., Jo, I., Park, J.W., Jung, S.C., et al. (2015). Tonsil-derived mesenchymal stem cells ameliorate CCl4-induced liver fibrosis in mice via autophagy activation. Sci. Rep. *5*, 8616.
34. Sato, Y., Araki, H., Kato, J., Nakamura, K., Kawano, Y., Kobune, M., Sato, T., Miyanishi, K., Takayama, T., Takahashi, M., et al. (2005). Human mesenchymal stem cells xenografted directly to rat liver are differentiated into human hepatocytes without fusion. Blood *106*, 756–763.
35. Mei, S.H., Haitsma, J.J., Dos Santos, C.C., Deng, Y., Lai, P.F., Slutsky, A.S., Liles, W.C., and Stewart, D.J. (2010). Mesenchymal stem cells reduce inflammation while enhancing bacterial clearance and improving survival in sepsis. Am. J. Respir. Crit. Care Med. *182*, 1047–1057.
36. Feng, J., Mantesso, A., De Bari, C., Nishiyama, A., and Sharpe, P.T. (2011). Dual origin of mesenchymal stem cells contributing to organ growth and repair. Proc. Natl. Acad. Sci. U S A *108*, 6503–6508.
37. Gatti, S., Bruno, S., Deregibus, M.C., Sordi, A., Cantaluppi, V., Tetta, C., and Camussi, G. (2011). Microvesicles derived from human adult mesenchymal stem cells protect against ischaemia-reperfusion-induced acute and chronic kidney injury. Nephrol. Dial. Transplant. *26*, 1474–1483.
38. Bruno, S., Grange, C., Deregibus, M.C., Calogero, R.A., Saviozzi, S., Collino, F., Morando, L., Busca, A., Falda, M., Bussolati, B., et al. (2009). Mesenchymal stem cell-derived microvesicles protect against acute tubular injury. J. Am. Soc. Nephrol. *20*, 1053–1067.
39. Yan, Y., Xu, W., Qian, H., Si, Y., Zhu, W., Cao, H., et al. (2009). Mesenchymal stem cells from human umbilical cords ameliorate mouse hepatic injury in vivo. Liver Int. *29*, 356–365.
40. Conde de la Rosa, L., Schoemaker, M.H., Vrenken, T.E., Buist-Homan, M., Havinga, R., Jansen, P.L., and Moshage, H. (2006). Superoxide anions and hydrogen peroxide induce hepatocyte death by different mechanisms: involvement of JNK and ERK MAP kinases. J. Hepatol. *44*, 918–929.
41. Clayton, A., Turkes, A., Dewitt, S., Steadman, R., Mason, M.D., and Hallett, M.B. (2004). Adhesion and signaling by B cell-derived exosomes: the role of integrins. FASEB J. *18*, 977–979.
42. Tan, C.Y., Lai, R.C., Wong, W., Dan, Y.Y., Lim, S.K., and Ho, H.K. (2014). Mesenchymal stem cell-derived exosomes promote hepatic regeneration in drug-induced liver injury models. Stem Cell Res. Ther. *5*, 76.
43. Smith, V.L., Jackson, L., and Schorey, J.S. (2015). Ubiquitination as a mechanism to transport soluble mycobacterial and eukaryotic proteins to exosomes. J. Immunol. *195*, 2722–2730.

44. Han, Y.H., Kim, H.J., Kim, E.J., Kim, K.S., Hong, S., Park, H.G., and Lee, M.O. (2014). RORα decreases oxidative stress through the induction of SOD2 and GPx1 expression and thereby protects against nonalcoholic steatohepatitis in mice. Antioxid. Redox Signal. *21*, 2083–2094.

45. Muller, A.S., and Pallauf, J. (2002). Down-regulation of GPx1 mRNA and the loss of GPx1 activity causes cellular damage in the liver of selenium-deficient rabbits. J. Anim. Physiol. Anim. Nutr. (Berl.) *86*, 273–287.

46. Cheng, W.H., Zheng, X., Quimby, F.R., Roneker, C.A., and Lei, X.G. (2003). Low levels of glutathione peroxidase 1 activity in selenium-deficient mouse liver affect c-Jun N-terminal kinase activation and p53 phosphorylation on Ser-15 in pro-oxidant-induced aponecrosis. Biochem. J. *370*, 927–934.

47. Koretsi, V., Kirschneck, C., Proff, P., and Römer, P. (2015). Expression of glutathione peroxidase 1 in the spheno-occipital synchondrosis and its role in ROS-induced apoptosis. Eur. J. Orthod. *37*, 308–313.

48. Wang, L., Huang, H., Fan, Y., Kong, B., Hu, H., Hu, K., Guo, J., Mei, Y., and Liu, W.L. (2014). Effects of downregulation of microRNA-181a on H2O2-induced H9c2 cell apoptosis via the mitochondrial apoptotic pathway. Oxid. Med. Cell. Longev. *2014*, 960362.

YMTHE, Volume *25*

Supplemental Information

hucMSC Exosome-Derived GPX1 Is Required for the Recovery of Hepatic Oxidant Injury

Yongmin Yan, Wenqian Jiang, Youwen Tan, Shengqiang Zou, Hongguang Zhang, Fei Mao, Aihua Gong, Hui Qian, and Wenrong Xu

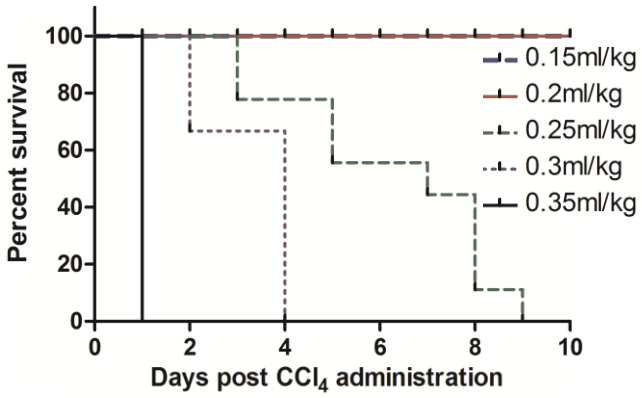

Fig.S1. Survival curves of CCl_4 injured mice received dosages between 0.15 and 0.35 mL/kg body wt by intraperitoneal injection.

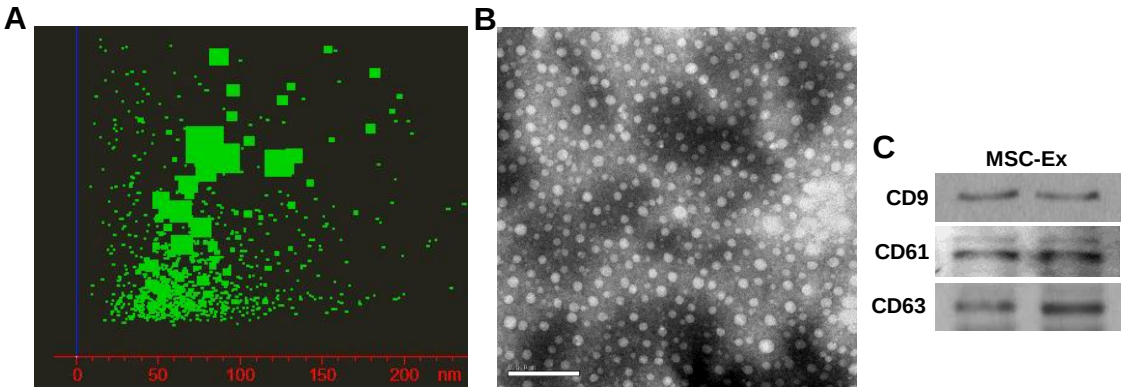

Fig.S2. HucMSC-Ex are detected by Nanoparticle Tracking Analysis (NTA) (A) and images under TEM are spheroid (scale bar 500 nm) (B). Western blot of CD9, CD61 and CD63 positive expression in hucMSC-Ex (C).

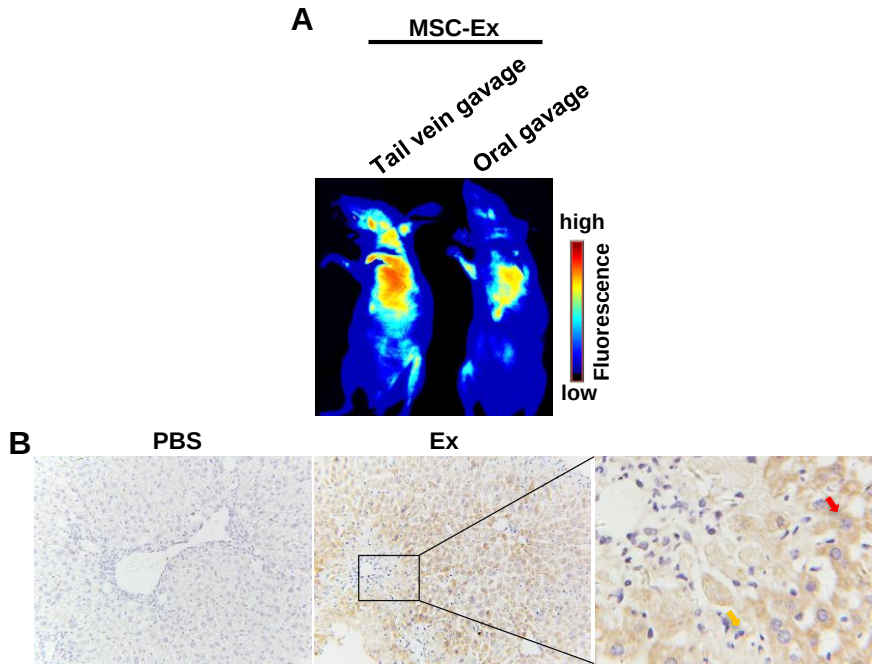

Fig.S3. Distribution of CM-Dir labeled hucMSC-Ex in normal mice after tail vein or oral gavage administration (A).Results showed that CM-Dir-labeled hucMSC-Ex administered by tail vein or oral gavage could target normal livers at 24 h post injection. CD63 staining of hucMSC-Ex in CCl_4 injured mouse liver; in each group 48 h after treatment (n = 3; *, P < 0.05; **, P < 0.01; ***, P < 0.001). (Red arrow: hepatocyte; Yellow arrow: Kupffer cells). Original magnification 200x (B).

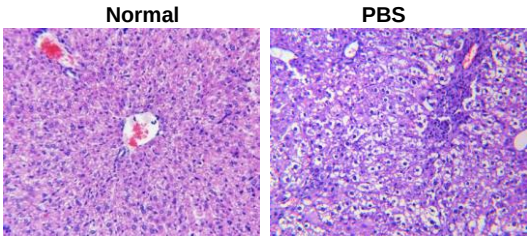

Fig.S4. Representative H&E images of mouse livers 72 h after PBS treatment. Original magnification 200x.Large areas of fatty degeneration and portal hepatocyte necrosis were induced in PBS treated mice.

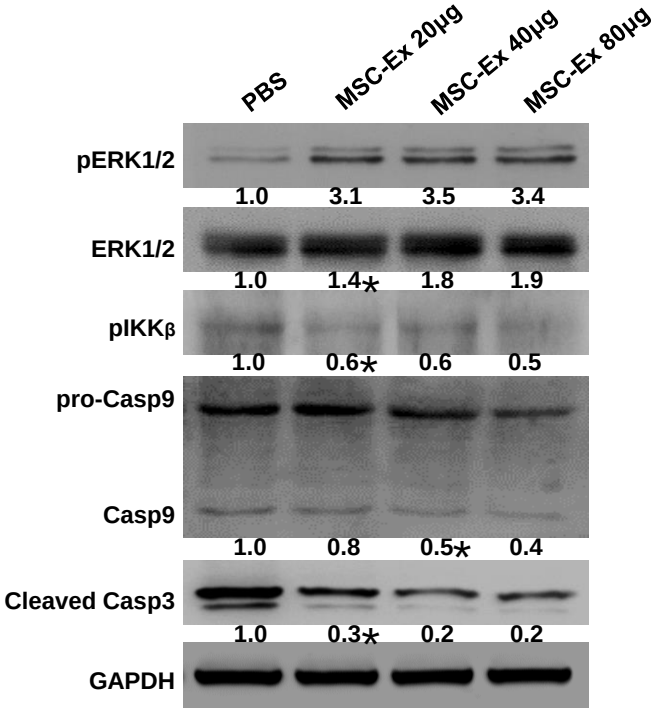

Fig.S5. Western blot quantification of pERK1/2, total ERK1/2, pIKKβ, casp9 and cleaved casp3 in CCl_4-injured L02 cells treated with PBS and hucMSC-Ex. he quantitated data expressed as relative ratio of specific proteins to GAPDH shown as numbers under individual blots (n = 3; *, P < 0.05).

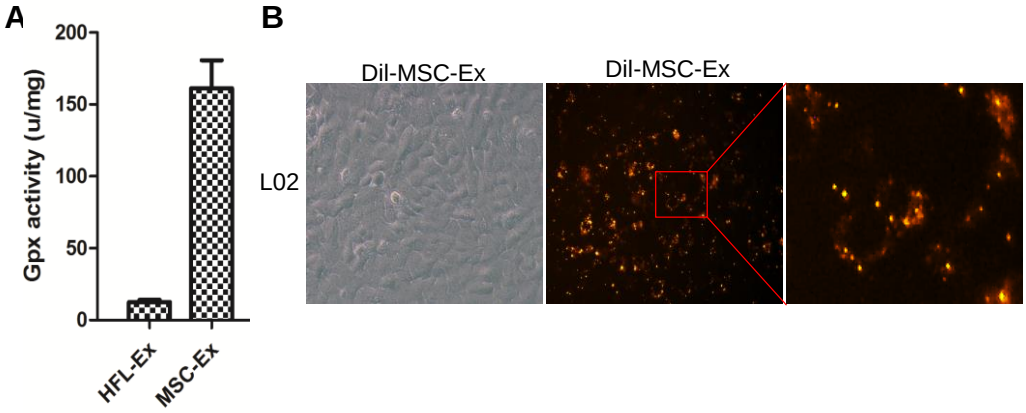

Fig.S6. Gpx activity of HFL-Ex and MSC-Ex. (n = 3) (A). Representative image of Dil labeled exosomes in L02 cells. Original magnification 200x. (B)

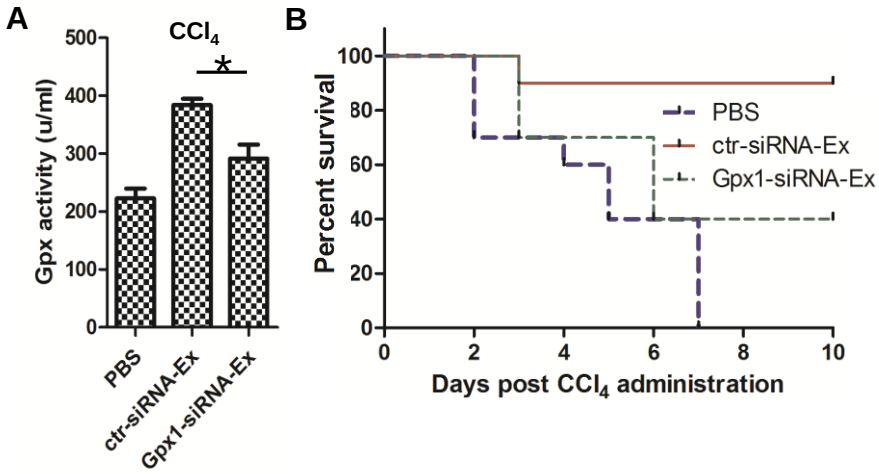

Fig.S7. Gpx activity of mice livers measured 48 h after PBS, ctr-siRNA-Ex or Gpx1-siRNA-Ex treatment. (n = 3; *, $P < 0.05$) (A). Survival curves of CCl_4 injured mice that underwent PBS, ctr-siRNA-Ex and Gpx1-siRNA-Ex administration by tail vein at 32mg/kg body weight (bt). (ctr-siRNA-Ex vs Gpx1-siRNA-Ex, n = 10, $P < 0.01$) (B). Gpx1 knockdown reduced Gpx activity in ex vivo hepatocytes (n = 3; *, $P < 0.05$) and attenuated the rescue of hucMSC-Ex on CCl_4 induced liver failure (n = 10; *, $P < 0.05$).